RSC Advances

Fabrication of Mn2O3 nanorods: An efficient catalyst for selective transformation of alcohol to aldehyde

Journal:	*RSC Advances*
Manuscript ID:	RA-ART-02-2015-002504.R2
Article Type:	Paper
Date Submitted by the Author:	21-Mar-2015
Complete List of Authors:	Rahaman, Hasimur; Department of Chemistry, Assam University, Laha, Radha; Department of Chemistry, University of Calcutta, Maita, Dilip; Department of Chemistry, University of Calcutta, Ghosh, Sujit; Assam University, Department of Chemistry

Cite this: DOI: 10.1039/c0xx00000x

www.rsc.org/Advances

PAPER

Fabrication of Mn_2O_3 nanorods: An efficient catalyst for selective transformation of alcohol to aldehyde

Hasimur Rahaman,[†] Radha M. Laha,[§] Dilip K. Maiti*[§] and Sujit Kumar Ghosh*[†]

Received (in XXX, XXX) Xth XXXXXXXXX 20XX, Accepted Xth XXXXXXXXX 20XX

DOI: 10.1039/b000000x

A facile wet chemical approach has been devised towards preparation of self-assembled high surface area nanostructured Mn_2O_3 through an effective polymer/surfactant interaction. Its outstanding catalytic property is discovered for selective transformation of alcohols to aldehydes. The polyethylene glycol/sodium dodecyl sulphate conjugates act as soft templates for the formation of manganese oxide nanorods upon treatment of a weak base, diethanolamine to manganese acetate precursor under mild refluxing conditions. The Mn_2O_3 nanorods were found as efficient and selective catalysts for synthesis of valuable aldehydes and ketones over undesirable acid byproduct using low catalyst loading. The precursor alcohols bearing activated and unactivated aromatic rings, double and triple bonds, and chiral sugar moiety were tolerated in this direct oxidative transformation strategy developed under benign reaction conditions.

1. Introduction

Catalyst is the work-horse in synthetic chemistry.[1-3] The robust reactivity and selectivity of catalyst lead to efficient transformation of raw materials into the desired pharmaceuticals, fuels, agrochemicals, pigments, polymers, commercial and natural compounds, which are essential for our highly demanding modern society. In this context, nanomaterials have tremendous potential to serve as significantly improved catalysis performance because of their active surface and interfacial atom effect, innovative new chemical property, high reactivity, low catalyst loading, environmentally benign nature, easy recovery and reusability.[4-20] In recent years, size and shape-controlled synthesis of manganese oxides (MnO_x) nanomaterials has fascinated considerable interest from both academia and industry due to tuneable physicochemical properties,[9-12] high-density magnetic storage media,[13] ion-exchange,[14] molecular adsorption,[15] electronics,[16] biosensors,[17] energy storage,[18] batteries[19] and catalysts.[20] Manganese oxides are the most attractive inorganic materials owing to their structural flexibility and availability of different oxidation states of manganese (II, III, IV) that have envisaged their structural, transport and magnetic properties[21-24] in a diverse range of niche applications.[25-27] Among the different oxidation states of manganese oxides, Mn_2O_3 is well known as cheap and environment-friendly catalyst and could be employed as ideal candidate for the removal of CO and NO_x from waste gas,[28] decomposition of H_2O_2 into hydroxyl radicals in the catalytic peroxidation of organic effluents[29] and as an oxygen storage component.[30] Although, catalytic activities over transition metal oxide catalysts are lower than those over noble metal catalysts, the inherent advantages of metal oxide catalysts, such as, low cost, high thermal stability, and high mechanical strength, which make them a promising alternative for outstanding catalytic applications.[3] While the catalytic activity of these materials at the nanoscale dimension depends strongly on their surface properties, the reactivity and selectivity of nanoparticles can be tuned through controlling the morphology because the exposed surfaces of the particles have distinct crystallographic planes depending on their shape.[32] Therefore, synthesis of Mn_2O_3 nanoparticles with well-controlled morphology and a narrow size distribution is desirable for achieving practical applications, such as, catalysis.

Diverse synthetic approaches have been implemented in the literature for the fabrication of size and shape-selective Mn_2O_3 nanostructures and exploited their physical and chemical properties in a wide range of applications. Ganguli and co-authors prepared nanorods of anhydrous manganese oxalate as precursor to synthesize single phase nanoparticles of various manganese oxides, such as, MnO, Mn_2O_3 and Mn_3O_4 under specific reaction conditions and studied their field-dependent magnetization properties.[33] Han and co-workers have reported the synthesis of Mn_2O_3 nanocrystals by the thermolysis of manganese(III) acetyl acetonate on a mesoporous silica, SBA-15 and the nanocomposites showed significant catalytic activity toward CO oxidation below 523 K.[34] Chen and He have described facile synthesis of mono-dispersed Mn_2O_3 nanostructures by treating a mixture of $KMnO_4$ solution and oleic acid at low temperatures (below 200 °C) and shown the application of these particles as efficient water purifier.[35] Polshettiwar and colleagues have

[†]*Department of Chemistry, Assam University, Silchar-788011, India Fax: +91-3842-270802; Tel: +91-3842-270848; e-mail: sujit.kumar.ghosh@aus.ac.in*

[§]*Department of Chemistry, University of Calcutta, Kolkata-700009, India e-mail: dkmchem@caluniv.ac.in*

devised a simple strategy using aqueous solution of $K_3[Mn(CN)_6]$ under microwave irradiation to afford the nanomaterial.[12] Gnanam and Rajendran have described the preparation of α–Mn_2O_3 nanoparticles by dropwise addition of an aqueous ammonia solution to manganese(II) chloride tetrahydrate ($MnCl_2.4H_2O$) in methanol under vigorous stirring and reported the optical properties of the synthesized materials.[36] Yang and colleagues reported the size-controlled synthesis of monodispersed Mn_2O_3 octahedra assembled from nanoparticles by a mediated *N*,*N*-dimethylformamide solvothermal route and the particles were found to exhibit catalytic activity towards CO oxidation.[37] Qiu et al. have described the synthesis of hierarchically structured Mn_2O_3 nanomaterials with different morphologies and pore structures from precursor containing the target materials interlaced with the polyol-based organic molecules and examined their potential as anode materials for lithium ion batteries.[38] Cao et al. have reported large-scale Mn_2O_3 homogeneous core/hollow-shell structures with cube-shaped and dumbbell-shaped morphologies and the particles were found to exhibit excellent performance in waste water treatment.[39] Najafpour and colleagues have described the synthesis of nano-sized Mn_2O_3 particles by decomposition of aqueous solution of manganese nitrate at 100 °C and it was observed that the particles possessing catalytic activity towards water oxidation and epoxidation of olefins in the presence of cerium(IV) ammonium nitrate and hydrogen peroxide, respectively.[40] We envisioned fabrication of Mn_2O_3 nanorods by the soft-templated strategy which will provide roughened high surface area to offer an ideal platform for high and innovative chemical activity towards novel catalysis processes such as most demanding direct synthesis of aldehydes and ketones from alcohols under oxidative conditions.

Aldehydes are valuable compounds and one of the most frequently used ingredients of organic synthesis in industry and academia. Tremendous importance of this class of compounds is supported by development of enormous methodologies for their synthesis reported in the literature.[41-45] Direct oxidative transformation of alcohols to aldehydes is a fundamental organic reaction. This approach suffers from a serious drawback of generating large quantity of corresponding acid[43] as a by-product because transformation of acid from in situ generated desired aldehyde is energetically more facile than the oxidation of alcohol to aldehyde. Thus, with the advent of synthesising metallic nanomaterials silver, gold, palladium, ruthenium and platinum nanoparticles were utilized under basic and/or stringent reaction conditions for oxidation of alcohol to aldehyde.[44,45] To improve the substrate scope, selectivity and versatility in the catalytic dehydrogenation process we envisioned using calcined manganese oxide nanorods and λ^3-hypervalent iodane[46,47] as a stoichiometric oxidant under neutral and benign reaction conditions (Scheme 1). In this article, we have reported an innovative fabrication approach to rod-shaped Mn_2O_3 nanostructures using polymer/surfactant assembly as soft-template and their catalytic activity is discovered towards selective oxidation of alcohols to valuable aldehydes, chiral analogue and ketones using phenyliododiacetate [$PhI(OAc)_2$] as an oxidizing agent.

2. Experimental

2.1 Reagents and instruments

All the reagents used were of analytical reagent grade. Manganese(II) acetate tetrahydrate, diethanolamine (DEA), polyethylene glycol (PEG-400), sodium dodecyl sulphate (SDS) and phenyliodoacetate ($PhI(OAc)_2$) were purchased from Sigma Aldrich and were used without further purification. Double distilled water was used throughout the course of the investigation. The temperature was 298±1 K during the experiments.

Absorption spectra were measured in a Shimadzu UV-1601 digital spectrophotometer (Shimadzu, Japan) taking the sample in 1 cm well-stoppered quartz cuvette. The surface and structural morphologies of Mn_2O_3 samples were studied by scanning electron microscopic (SEM) images were recorded by using JSM-6360 (JEOL) instrument equipped with a field emissioncathode with a lateral resolution of approximately 3 nm and acceleration voltage 3 kV after sputtering the sample on silicon wafer with carbon (approx. 6 nm). Thin films were prepared by drop-coating from the aqueous-methanolic solutions of the respective samples onto silicon wafers. Transmission electron microscopy was carried out on a JEOL JEM-2100 microscope with a magnification of 200 kV. Samples were prepared by placing a drop of solution on a carbon coated copper grid and dried overnight under vacuum. High-resolution transmission electron micrographs and selected area electron diffraction (SAED) pattern were obtained using the same JEOL JEM-2010, operating at 200 kV. Energy dispersive X-ray (EDX) analysis was performed on an INCA Energy TEM 200 using an X-ray detector. Fourier transform infrared (FTIR) spectra were recorded in the form of pressed KBr pallets in the range (400-4000 cm^{-1}) with Shimadzu-FTIR Prestige-21 spectrophotomèter. The powder X-ray diffraction patterns were obtained using a D8 Advanced Broker axs X-ray Diffractometer with CuK_α radiation (λ = 1.540589 Å); data were collected at a scan rate of 0.5° min^{-1} in the range of 10º-80º. Raman scattering measurements are carried out on silicon substrate in backscattering geometry using a fiber-coupled micro-Raman spectrometer equipped with 488 nm (2.55 eV) of 5 mW air cooled Ar^+ laser as the excitation light source, a spectrometer (model TRIAX550, JY) and a CCD detector. The powder specific surface area was measured by BET analysis using a Micromeritics Tristar 3000 surface area analyzer. Thermogravimetric analysis was carried out on a Perkin-Elmer STA 6000 with the sample amount of 10 mg. The measurements were performed under nitrogen with heating from 40-800 ºC (rate: 10 ºC min^{-1}) and then, maintained at 800 ºC for half an hour. Before TGA measurements, the samples were dried overnight in vacuum oven at 50 ºC.

2.2 Synthesis of manganese oxide nanorods in polymer-surfactant conjugates

The nanostructures of manganese oxide have been synthesised using polymer-surfactant conjugates and manganese acetate tetrahydrate as the precursor salt. In a typical synthesis, an aliquot of aqueous polyethylene glycol (PEG) (0.4 mmol dm^{-3}) was added to an aqueous solution of sodium dodecyl sulphate (SDS)

(2 mmol dm^{-3}) in a double-naked round-bottom flask so that the total volume of the solution is 25 mL and the mixture was stirred overnight at room temperature. Now, an amount of 0.245 g $Mn(ac)_2.4H_2O$ was dissolved in the polymer-surfactant mixture by refluxing on a water bath at 65°C. After complete dissolution of the precursor, 100 µL diethanolamine was added and refluxing was continued for another 6 h. After about 30 min, the reaction mixture, suddenly, turned into yellowish brown from a colourless solution indicating the formation of manganese oxide nanostructures. As the refluxing was continued, the colour slowly changed into deep brown pointing out to the aggregation between the ultrasmall manganese oxide particles to rod shaped nanostructures. The water-bath was removed and the reaction mixture was stirred for 12 h at room temperature. The particles formed by this method was washed five times with slightly hot water and finally, dispersed in water. The manganese oxide nanostructures prepared by this method are stable for a month and can be stored in the vacuum desiccator without any significant agglomeration or precipitation of the particles.

2.3 General procedure for synthesis of aldehydes

The precursor alcohol (1 mmol), Mn_2O_3 (1.6 mg, 0.01 mmol), $PhI(OAc)_2$ (403 mg, 1.25 mmol) and $MgSO_4$ (about 300 mg) were taken together in ethylenedichloride (EDC, 25 mL) and stirred magnetically at 45 °C until the reaction was complete. The progress of the reaction was monitored by TLC. After completion of the reaction the post reaction mixture was filtered through a sintered funnel and the residue was washed with EDC (2×5 mL). The combined EDC was transferred to a separating funnel, washed with water (3×10 mL) and dried using activated $MgSO_4$. The solvent was removed in a rotary evaporator at room temperature under reduced pressure. The crude product was purified by column chromatography over silica gel (60–120 mesh) using ethyl acetate-petroleum ether as eluent to afford the desired aldehyde and corresponding acid byproduct. Thus, the reaction of benzyl alcohol (1a, 109 mg, 1.0 mmol) afforded benzaldehyde (2a) and benzoic acid (3a) after purification by column chromatography on silica gel (60-120 mesh) with ethyl acetate-petroleum ether (1:200, v/v) as an eluent in an yield of 87% (92.5 mg, 0.87 mmol) and 4% (4.5 mg, 0.04) respectively. The structure of the desired product (2a) and byproduct (3a) were confirmed with the help of the available literature boiling and melting points and also comparing the recorded NMR (^1H and ^{13}C), FT-IR, and mass (HR-MS) spectra. Similarly other aldehydes (2b-e), ketones (4a,b), acids (3a-f) and sugar aldehyde (2f) were characterized by measuring melting/boiling points, recording NMR (^1H and ^{13}C), FT-IR, and mass (HR-MS) spectra and optical rotation, which were verified with the know literature data and spectra.

3. Results and discussion

In the present experiment, we have reported an innovative fabrication approach to rod-shaped Mn_2O_3 nanostructures using polymer/surfactant assembly as soft-template and their catalytic activity is discovered towards selective oxidation of alcohols to valuable aldehydes, chiral analogue and ketones using phenyliododiacetate [$PhI(OAc)_2$] as an oxidizing agent.

The absorption spectral features of the as-synthesized Mn_2O_3 sample in the solid state are shown in ESI 1. The estimated direct band gap of the Mn_2O_3 was found to be 1.29 eV; this value is almost close to reported value of the Mn_2O_3 nanostructures.[48] The morphology, composition and crystallinity of the particles synthesized in the polymer/surfactant mixture are presented in Fig. 1. Representative scanning electron micrograph (trace a) of the Mn_2O_3 particles shows bunch of elongated nanorods with length up to 1±0.3 µm and width 50±10 nm. To further examine the surface morphology of the microstructures, high magnification SEM images were recorded (trace b) and it was apparent that the surface of the particles was with roughened edge, which indicates the growth and slow transformation to rod-shaped nanostructures occur through oriented aggregation of primary nanocrystals. At the very beginning of reflux, the concentration of reactants is comparatively high; therefore, some nuclei can be formed very fast resulting in the occurrence of ultrasmall particles. The nuclei, subsequently, orient and grow fast along the (211) direction to form one dimensional nanorods.[49] The size and shape of the nanocrystals is further

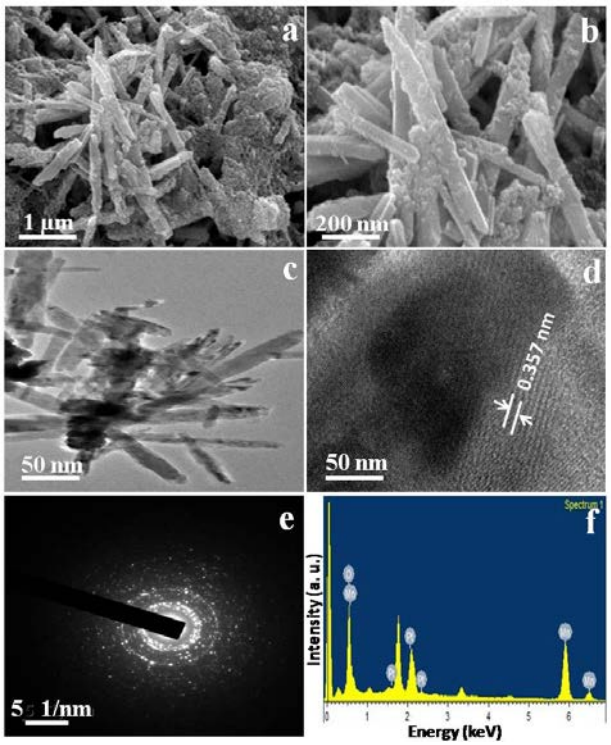

Fig. 1. (a) Scanning electron micrograph, (b) high resolution scanning electron micrograph, (c) transmission electron micrograph, (d) high resolution transmission electron micrograph, (e) selected area electron diffraction pattern, and (e) energy dispersive X-ray analysis of themanganese oxide microrods in polymer-surfactant conjugates.

evident from the transmission electron micrographs (panel c) of the Mn_2O_3 particles formed in the polymer/surfactant assembly. High resolution TEM image (panel d) of the Mn_2O_3 nanoorods displays the interplanar distance between the fringes about 0.357 nm which corresponds to the distance between the (211) planes of the Mn_2O_3 crystal lattice.[50] Selected area electron diffraction pattern (panel e) of the Mn_2O_3 nanostructures is consistent with

strong ring patterns due to (211), (222) and (400) planes and therefore, confirms the crystallinity of the materials.[51] Representative energy dispersive X-ray spectrum (panel f) of Mn_2O_3 nanorods indicates that the particles are composed of Mn and O elements. The formation of manganese oxide particles in the polymer-surfactant conjugates has been studied through FTIR spectroscopy (ESI 2). It is seen that the Mn–O bond stretching frequency appears in the range of 450–680 cm^{-1} along with two strong peaks at 630 and 525 cm^{-1} that arise due to the stretching vibration of Mn–O and Mn–O–Mn bonds,[35] indicating the formation of Mn_2O_3 in the polymer/surfactant conjugates.[52] The X-ray diffraction pattern of the of the representative hybrid rod-shaped assemblies is shown in ESI 3; all diffraction peaks implying a crystalline structure are consistent with the standard values of bulk Mn_2O_3 [JCPDS No-41-1442].[34] Fig. 2 shows the Raman spectrum of the as-prepared nanorods under ambient condition. The structure of Mn_2O_3 belongs to Ia_3 symmetry group with a = 9.41 and possess cubic bixbyite structures.[53] The bands at 310, 366 and 655 cm^{-1} could be ascribed to the out of-plane bending modes of Mn_2O_3, the asymmetric stretch of bridge oxygen species (Mn–O–Mn) and the symmetric stretch of Mn_2O_3 respectively[54, 55] in correspondence to that obtained for bulk MnO*x* particles.[56]

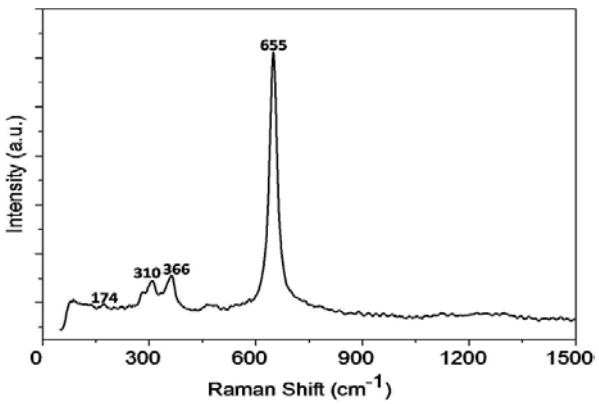

Fig. 2. Raman spectrumof the manganese oxide/polymer-surfactant hybrid assemblies dried in air.

Thermogravimetric analysis (ESI 4) of the as-dried powder sample shows two weight loss steps in the curve: 8.9 wt% loss corresponding to the water desorption (up to 200 °C), and a weight loss of 32.1 wt % over 200-800 ºC as a result of the decomposition of polymer/surfactant assemblies, verifying that the polymer/surfactant conjugates are, indeed, incorporated into the nanostructures.[57] The textural properties of the Mn_2O_3 microrods were investigated by Brunauer–Emmett–Teller (BET) gas-sorption measurements performed at 77 °K of the as-dried powder sample under vacuum as shown in ESI 5. The specific surface area and Langmuir surface area of the microrods have been measured to be *ca.* 13.60 m^2 g^{-1} and 22.27 m^2 g^{-1}, respectively from which it is evident that Mn_2O_3 nanorods, synthesised in the present experiment, manifest high BET surface areas to provide a platform for the catalytic organic transformation.[30,58]

In the initial experiments, we have decided not to apply high temperature for the desired catalytic oxidation (Scheme 1) of our

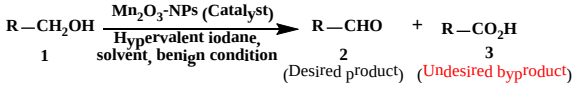

Scheme 1. Direct synthesis of aldehydes using Mn_2O_3-nanorods catalyst

model substrate benzylalcohol (**1a**, R= Ph, shown in ESI 6) to benzaldehyde (**2a**) using λ^3-hypervalent iodane,[46,47,59] so that the possibility of forming byproduct benzoic acid (**3a**, entry 1, Table 1) could be avoided. After several experiments using as-synthesised Mn_2O_3 nanorods (1 mol%) we discovered its catalytic property for the oxidative dehydrogenation reaction using PhIO[46] (1.25 mmol), which revealed about 60% conversion at 50 °C to afford benzaldehyde (**2a**; yield: 45%) with high selectivity (**2a**:**3a** = 9:1). The yield (68%) was improved on use of $PhICl_2$ (entry 2). Gratifyingly utilizing commercially available $PhI(OAc)_2$[47] the conversion (100%), reaction rate (2 h), yield (96%) and selectivity (**2a**:**3a** = 47:3) were significantly improved under the similar reaction conditions (entry 3). The optimized oxidation process was found utilizing as low as 0.01 mol% of the nanorods as described in the entry 7, which was obtained (entries 5-8) by changing the reaction temperature (50-40 °C) and catalyst loading (1-0.005). The reaction rate (70% in 12 h), yield (48%) and selectivity (**2a**:**3a** = 2:3) were drastically reduced in absence of the Mn_2O_3-NPs (entry 9). Ethylene dichloride was found as the suitable solvent because the other polar aprotic solvents such as dichloromethane (CH_2Cl_2), tetrahydrofuran (THF) and acetonitrile (entries 10-12), nonpolar toluene (entry 13) and protic methanol or water (entries 14,15) were not effective for the unprecedented catalytic process.

The diverse catalytic activity of the Mn_2O_3-nanorods was evaluated utilizing various types of alcohols under the optimized reaction conditions (entry 1, Table 2 as shown in ESI 6). The benzyl alcohols bearing activated (**1b**) and deactivated (**1c**) aromatic moiety (entries 2,3, Table 2) were tolerated in this reaction to afford corresponding aldehyde with excellent yield and selectivity (entries 2,3). Interestingly in presence strongly electron withdrawing -NO_2 group the reaction rate was enhanced (from 4.5 to 3 h) with respect to activated aromatic nucleus (**1b**), which simultaneously reduced the selectivity from 19:1 to 23:2 (entries 2,3).

The diverse catalytic activity of the Mn_2O_3-nanorods was evaluated utilizing various types of alcohols under the optimized reaction conditions (entry 1, Table 2). The benzyl alcohols bearing activated (**1b**) and deactivated (**1c**) aromatic moiety (entries 2,3, Table 2) were tolerated in this reaction to afford corresponding aldehyde with excellent yield and selectivity (entries 2,3). Interestingly in presence strongly electron withdrawing -NO_2 group the reaction rate was enhanced (from 4.5 to 3 h) with respect to activated aromatic nucleus (**1b**), which simultaneously reduced the selectivity from 19:1 to 23:2 (entries 2,3). Another interesting feature observed in this reaction is the high chemoselectivity. Even in presence of oxidation prone double and triple bond-bearing allyl (**1d**) and propargyl (**1e**) alcohols (entries 4,5) smoothly underwent oxidation to

Table 1. Synthesized aldehydes, sugar aldehyde and ketones

Entry	Alcohol(1)	Catalyst	Reagent &conditions	Conversion (%)	Desired aldehyde(2) or ketone (4)	Acid(3)	Yield(%, 2:3)
1	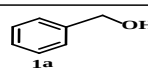 1a	Mn_2O_3 (0.01 mol%)	$PhI(OAc)_2$, EDC, 45 °C 4.0 h	100	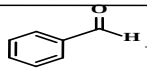 2a:96%	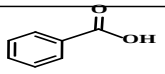 3a:4%	91 (24:1)
2	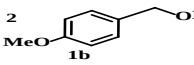 1b	Mn_2O_3 (0.01 mol%)	$PhI(OAc)_2$, EDC, 45 °C 4.5 h	100	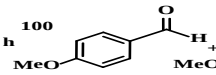 2b:95%	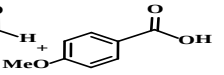 3b:5%	89 (19:1)
3	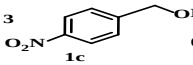 1c	Mn_2O_3 (0.01 mol%)	$PhI(OAc)_2$, EDC, 45 °C 3.0 h	100	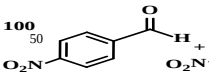 2c: 92%	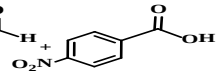 3c: 8%	95 (23:2)
4	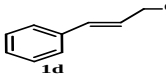 1d	Mn_2O_3 (0.01 mol%)	$PhI(OAc)_2$, EDC, 45 °C 4.0 h	100	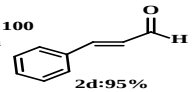 2d:95%	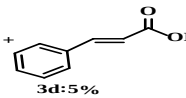 3d:5%	90 (19:1)
5	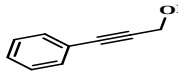 1e	Mn_2O_3 (0.01 mol%)	$PhI(OAc)_2$, EDC, 45 °C 4.0 h	100	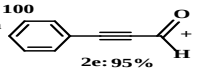 2e: 95%	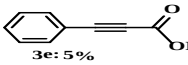 3e: 5%	92 (19:1)
6	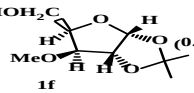 1f	Mn_2O_3 (0.01 mol%)	$PhI(OAc)_2$, EDC, 45 °C 4.0 h	100	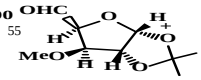 2f: 91%	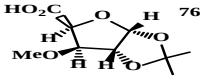 3f: 9%	76 (91:9)
7	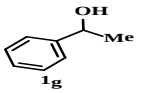 1g	Mn_2O_3 (0.02 mol%)	$PhI(OAc)_2$, EDC, 45 °C 6.0 h	100	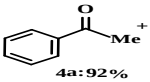 4a:92%	3a (Not detected)	
8	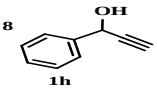 1h	Mn_2O_3 (0.02 mol%)	$PhI(OAc)_2$, EDC, 45 °C 5.0 h	100	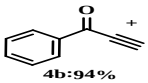 4b:94%	3a (Not detected)	

corresponding aldehydes with 90-92% yield and outstanding selectivity (19:1). We turned our attention applying the benign strategy for oxidation of sugar-based chiral alcohol (**1f**, entry 6) and under the similar reaction conditions it afforded corresponding optically pure aliphatic aldehyde (**2f**) with high yield (76%) and selectivity (91:9). The diverse catalytic activity of the Mn_2O_3-nanorods was also successfully exploited on functionalized secondary alcohols (**1g**, **1h**) to obtain corresponding ketons (**4a**, **4b**, entries 8,9) without formation of the byproduct benzoic acid (**3a**). The catalytic reaction was tested with bulk Mn_2O_3 and it was seen that the particles could not selectively transform the alcohols to aldehydes. A comparative account highlighting utility of Mn_2O_3 nanorods and some other catalysts[60-63] towards the oxidation of alcohols is presented in ESI 7. This unprecedented property of Mn_2O_3-nanorods under very low catalyst loading (0.01 mol%) provides new prospects and perspectives in catalysis towards discovery of new materials, innovative catalytic activity and novel organic transformation to afford functional molecules for our highly demanding modern society.

4. Conclusion

In conclusion, hydrolysis of manganese precursor in the presence of polymer/surfactant soft template has been found to be an effective strategy for the fabrication of Mn_2O_3 nanorods. The nanorods are crystalline and offer roughen surface and large surface area that installs new and innovative catalytic activity such as direct synthesis of valuable aldehydes through oxidation of alcohols in a highly chemoselective fashion. This new synthetic strategy for low dimensional manganese oxide material could be exploited for fabrication of novel inorganic materials with controlled superstructures and unusual functionalities. This unprecedented catalytic activity of Mn_2O_3 nanorods provides new prospects and perspectives in catalysis for the pursuance of novel organic transformations to afford functional molecules for our highly demanding modern society.

Acknowledgement

We gratefully acknowledge financial support from DBT, New Delhi (project No. BT/277/NE/TBP/2013) and DST, Nanomission, Govt. of India (project no. SR/NM/NS-29/2010). We are also thankful to CRNN, University of Calcutta for providing microscope facility to analyse the Mn_2O_3-microrods.

Supporting Information. Characterization details of synthesized materials, reaction schemes, catalysis details with tables. This material is available free of charge at http://www.rsc.org.

References

1. G. Rothenberg, Catalysis (Wiley, VHC, Weinheim, 2008).
2. M. Peplow, *Nature* 2013, **495**, S10–S11.
3. S. Ghosh, S. Khamarui, K. S. Gayen, D. K. Maiti, *Sci. Rep.* 2013, **3**, 2987 (1-7).
4. M. Turner, V. B. Golovko, O. P. H. Vaughan, P. Abdulkin, A. Berenguer-Murcia, M. S. Tikhov, B. F. G. Johnson, R. M. Lambert, *Nature* 2008, **454**, 981–984.

5. K. S. Gayen, T. Sengupta, Y. Saima, A. Das, D. K. Maiti, A. Mitra, *Green Chem.*2012, **14**, 1589–1592.
6. V. Polshettiwar, J. -M. Basset, D. Astruc *ChemSusChem* 2012, **5**, 6–8.
7. B. C. Ranu, D. Saha, D. Kundu, N. Mukherjee, in *Nanocatalysis: Synthesis and Applications* of *Aryl Carbon-Heteroatom Coupling Reactions using Nano-Metal Catalyst* (eds. V. Polshettiwar, T. Asefa, Wiley–VCH, 2013).
8. R. S. Varma, *Sustainable Chemical Processes* 2014, **2,** 11 (1–8).
9. Z. Chen, Z. Jiao, D. Pan, Z. Li, M. Wu, C. –H. Shek, C. M. L. Wu, K. L. L. Joseph, *Chem. Rev.*2012, **112**, 3833–3855.
10. W. Weifeng, C. Xinwei, C. Weixing, G. I. Douglas, *Chem. Soc. Rev.* 2011, **40**, 1697–1721.
11. G. S. Thomas, J. R. Bargar, S. Garrison, M. T. Bradley, *Acc. Chem. Res.*2010, **43**, 2–9.
12. V. Polshettiwar, B. Baruwati, R. S. Varma *ACS Nano* 2009, **3**, 728–736.
13. Z. Hao, C. Gaoping,W. Zhiyong,Y. Yusheng, S. Zujin, G. Zhennan, *Nano Lett.* 2008, *8*, 2664–2668.
14. Y. Hirao, C. Yokoyama, M. Makoto, *Chem. Commun.* 1996, 597–598.
15. E. A. Kotomin, Y. A. Mastrikov, E. Heifets, J. Maier, *Phys. Chem. Chem. Phys*. 2008, *10*, 4644–4649.
16. Z. W. Chen, S. Y. Zhang, S. Tan, J. Wang, S. Z. Jin, *Appl. Phys. A* 2004, **78**, 581–584.
17. S. Huang, Y. Ding, Y. Liu, L. Su, R. Filosa Jr. Y. Lei, *Electroanalysis* 2001, **23**, 1912–1920.
18. J. –H. Kim, K. H. Lee, L. J. Overzet, G. S. Lee, *Nano Lett.* 2011, **11**, 2611–2617.
19. M. M. Thackeray, C. S. Johnson, J. T. Vaughey, N. Li, S. A. Hackney, *J. Mater. Chem.* 2005, **15**, 2257–2267.
20. O. Giraldo, S. L. Brock, W. S. Willis, M. Marquez, S. L. Suib, *J. Am. Chem. Soc.* 2000, **122**, 9330–9331.
21. S. K. Nayak, P. Jena, *Phys. Rev. Lett.* 1998, **81**, 2970–2973.
22. E. Lidstrom, O. Hartmann, *J. Phys: Condens. Matter*. 2000, **12**, 4969–4974.
23. J. E. Pask, D. J. Singh,I. I. Mazin, C. S. Hellberg, J. Kortus, *Phys. Rev. B* 2001, **64**, 024403 1–3.
24. I. Djerdj, D. Arčon, Z. Jagličić, M. Niederberger, *J. Phys. Chem. C* 2007, **111**, 3614–3623.
25. R. Ma, Y. Bando, L. Zhang, T. Sasaki, *Adv. Mater*. 2004, **16**, 918–922.
26. F. Y. Cheng, J. A. Shen, B. Peng, Y. D. Pan, Z. L. Tao, *J. Chen, Nature Chem.* 2011, **3**,79–84.
27. Y. Oaki, H. Imai, *Angew. Chem. Int. Ed.* 2007, **119**, 5039–5043.
28. H.M. Zang, Y. Teraoka, *Catal. Today* 1989, **6**, 155–162.
29. B. Ammundsen, J. Paulsen, *Adv. Mater*. 2001, **13**, 943–956.
30. Y. F. Chang, J. C. McCarty, *Catal. Today* 1996, **30**,163–170.
31. P. Serp, K. Philippot, G. A. Somorjai, B. Chaudret, *Nanomaterials in Catalysis*, Wiley-VCH, Winheim, Germany, 2013.
32. L. Hu, Q. Peng, Y. Li, *J. Am. Chem. Soc.* 2008, **130**, 16136–16137.
33. A. Tokeer, K. V. Ramanujachary, S. E. Lofland, G. Ashok, *J. Mater. Chem.* 2004, **14**, 3406–3410.
34. Y. –F. Han, F. Chen, Z. Zhong, K. Ramesh, L. Chen, E. Widjaja, *J. Phys. Chem. B* 2006, **110**, 24450–24456.
35. C. Hongmin, H. Junhui, *J. Phys. Chem. C* 2008, **112**, 17540–17545.
36. S. Gnanam, V. Rajendran, *J. Sol-Gel Sci. Technol.* 2011, **58**, 62–69.
37. L. Liu, H. Liang, H. Yang, J. Wei, Y. Yanzhao, *Nanotechnology* 2011, **22**, 015603–015611.
38. Y. Qiu, G. –L. Xu, K. Yan, H. Sun, J. Xiao, S. Yang, S. –G. Sun, L. Jin, H. Deng *J. Mater. Chem.*, 2011, **21**, 6346–6353.
39. J. Cao, Q. Mao, Y. Qian, *J. Solid State Chem.* 2012, **191**, 10–14.
40. M. Amini, M. M. Najafpour, S. Nayeri, B. Pashaei, M. Bagherzadeh, *Dalton Trans.* 2012, **41**, 11026–11031.
41. T. Mallat, A. Baiker, *Chem. Rev.* 2004, **104**, 3037–3058.
42. C. J. Weiss, P. Das, D. L. Miller, M. L. Helm, A. M. Appel, *ACS Catal*. 2014, **4**, 2951–2958.
43. D. Könning, T. Olbrisch, F. D. Sypaseuth, C. C. Tzschucke, M. Christmann, *Chem. Commun*. 2014, **50**, 5014–5016.
44. Y. Hong, X. Yan, X. Liao, R. Li, S. Xu, L. Xiao, J. Fan, *Chem. Commun.* 2014, **50**, 9679–9682.
45. Z. -A. Qiao, P. Zhang, S. –H. Chai, M. Chi, G. M. Veith, N. C. Gallego, M. Kidder, S. Dai, *J. Am. Chem. Soc.* 2014, **136**, 11260–11263.
46. D. K. Maiti, N. Chatterjee, P. Pandit, S. K. Hota, *Chem. Commun.* 2010, **46**, 2022–2024.
47. S. Khamarui, R. Maiti, D. K. Maiti, *Chem. Commun.* 2015, **51**, 384–387.
48. Q. Javed, F. –P. Wang, M. Y. Rafique, A. M. Toufiq, M. Z. Iqbal, *Chinese Phys. B.* 2012, **21**, 117311 1–7.
49. Y. Li, H. Tan, O. Lebedev, J. Verbeeck, E. Biermans, G. van Tendeloo, B. –L. Su, *Cryst. Growth Des.* 2010, **10**, 2969–2976.
50. G. Yang, W. Yan, J. Wang, H. Yang, *Cryst. Eng. Comm.* 2014, **16**, 6907–6913.
51. L. Ling, L. Hui, Y. Hongxiao, W. Jingjing, Y. Yanzhao, *Nanotechnology* 2011, **22**, 015603–015611.
52. S. K. Ghosh, M. Ali, H. Chatterjee, *Chem. Phys. Lett.* 2013, **561**, 147–152.
53. C. M. Julien, M. Massot, C. Poinsignon, *Spectrochim. Acta A* 2004, **60**, 689–700.
54. Y. T. Chua, P. C. Stair, I. E. Wachs, *J. Phys. Chem. B* 2001, **105**, 8600–8606.
55. F. Buciuman, F. Patcas, R. Cracium, D. R. T. Zahn, *Phys. Chem. Chem. Phys.* 1999, **1**, 185–190.
56. Y. Luo, Y. –Q. Deng, W. Mao, X. –J. Yang, K. Zhu, J. Xu, Y.-F. Han, *J. Phys. Chem. C* 2012, **116**, 20975–20981.
57. H. –P. Cong, S. -H. Yu, *Adv. Funct. Mater.* 2007, **17**, 1814–1820.
58. S. Brunauer, P. H. Emmett, E. Teller, *J. Am. Chem. Soc.* 1938, **60**, 309–319.
59. M. Uyanik, K. Ishihara, *Chem. Commun.* 2009, 2086–2099.
60. J. Zhu, K. Kailasam, A. Fischer, A. Thomas, *ACS Catal*. 2011, **1**, 342–347.
61. H. Caot, S. L. Suib, *J. Am. Chem. Soc.* 1994,**116**, 5334–5342.
62. X. Fu, J. Feng, H. Wang, K. M. Ng, *Nanotechnology*, 2009, **20**, 375601–375610.
63. J. Chen, J. C. Lin, V. Purohit, M. B. Cutlip, S. L. Suib *Catal. Today* 1997, **33**, 205–214.